nature immunology

The transcription factor Zbtb32 controls the proliferative burst of virus-specific natural killer cells responding to infection

Aimee M Beaulieu[1], Carolyn L Zawislak[1], Toshinori Nakayama[2] & Joseph C Sun[1]

Natural killer (NK) cells are innate lymphocytes that exhibit many features of adaptive immunity, including clonal proliferation and long-lived memory. Here we demonstrate that the BTB-ZF transcription factor Zbtb32 (also known as ROG, FAZF, TZFP and PLZP) was essential for the proliferative burst and protective capacity of virus-specific NK cells. Signals from proinflammatory cytokines were both necessary and sufficient to induce high expression of Zbtb32 in NK cells. Zbtb32 facilitated NK cell proliferation during infection by antagonizing the anti-proliferative factor Blimp-1 (*Prdm1*). Our data support a model in which Zbtb32 acts as a cellular 'hub' through which proinflammatory signals instruct a 'proliferation-permissive' state in NK cells, thereby allowing their prolific expansion in response to viral infection.

NK cells are critical mediators of host immunity to malignancy and viral infection. Activation of NK cells is primarily controlled by germ line–encoded surface receptors that recognize self-encoded or virally encoded molecules expressed on infected or stressed cells and by proinflammatory cytokines, such as interleukin 12 (IL-12), IL-18 and type I interferons (IFNs). Activated NK cells respond by proliferating and by rapidly secreting cytokines such as IFN-γ and tumor necrosis factor (TNF) and cytotoxic molecules (perforin and granzyme B) that lyse infected or malignant target cells[1].

Although classically NK cells have been considered cells of the innate immune system, they are now appreciated to have a number of developmental and effector function features in common with T cells and B cells of the adaptive immune system. Similarities include development from a common lymphoid progenitor cell, a requirement for common γ-chain–dependent cytokines (for example, IL-15 and IL-7) during development and homeostasis, and an education process in the bone marrow that is analogous to T cell development in the thymus[1]. Moreover, much like their B cell and T cell counterparts, which use the B cell antigen receptor and T cell antigen receptor (TCR), respectively, to recognize antigens, NK cells also express activating receptors capable of directly binding foreign, often virally derived, antigens. For example, in C57BL/6 mice, the activating receptor Ly49H binds the mouse cytomegalovirus (MCMV)-encoded glycoprotein m157 (refs. 2,3); receptor-ligand engagement drives a proliferative 'burst' and effector response that is both necessary and sufficient for resistance to MCMV in this mouse strain[4–7]. Kinetics of the Ly49H$^+$ NK cell response to MCMV infection are highly reminiscent of antigen-specific B cell and T cell responses. Most notably, the primary response, which peaks in cell number at around day 7 after infection[7,8], contracts into a long-lived pool of antigen-specific NK cells that exhibit many features of immunological 'memory', including long-term persistence and enhanced functionality upon antigen rechallenge[8].

Broad complex, Tramtrack, Bric á brac and zinc finger (BTB-ZF) proteins are a large family of transcription factors with important roles in development, differentiation and oncogenesis[9]. Family members are characterized by the presence of C-terminal C_2H_2 Krüppel-type zinc finger domains, which facilitate sequence-specific DNA binding at target loci, and an N-terminal BTB domain that recruits co-repressors and histone modification enzymes to the site of regulation[9,10]. BTB-ZF proteins are currently thought to act primarily as repressors of target gene transcription, in part by modifying chromatin accessibility at target loci.

A growing number of studies have revealed an essential and nonredundant role for BTB-ZF proteins in the regulation of lineage commitment, development and effector function in lymphocytes[10]. Examples include LRF, which controls T cell versus B cell commitment[11]; MAZR and ThPOK, which direct CD8$^+$ and CD4$^+$ T cell lineage commitment, respectively[12–16]; PLZF, which regulates the development and function of NKT and γδ T cells[17–20]; and Bcl-6, which is required for formation of germinal-center B cells and follicular T helper cells[21–25]. The extent to which BTB-ZF proteins regulate NK cell development and function is largely unknown. Given their prominent role in T cell and B cell biology, we hypothesized that BTB-ZF proteins may act as important regulators of the adaptive lymphocyte–like features of NK cells. Here we identify the BTB-ZF transcription factor Zbtb32 as an essential regulator of the proliferative burst of MCMV-specific NK cells in response to viral infection *in vivo* and show that Zbtb32 is required for NK cell–mediated protection against lethal viral challenge.

[1]Immunology Program, Memorial Sloan-Kettering Cancer Center, New York, New York, USA. [2]Department of Immunology, Graduate School of Medicine, Chiba University, Chiba, Japan. Correspondence should be addressed to J.C.S. (sunj@mskcc.org).

Received 14 February; accepted 26 March; published online 20 April 2014; doi:10.1038/ni.2876

RESULTS

MCMV infection induces Zbtb32 expression in NK cells

To identify BTB-ZF genes that might regulate antigen-specific NK cell responses, we first compared expression of 47 BTB-ZF genes in sorted Ly49H$^+$ NK cells from MCMV-infected and uninfected mice by microarray. Only three (*Zbtb32*, *Hic1* and *Bcl6*) were significantly modulated in NK cells on day 1.5 after infection, and of these three, *Zbtb32* was the most highly upregulated (**Fig. 1a**). Of the >35,000 genes evaluated on the microarray (Gene Expression Omnibus: GSE15907)[26], *Zbtb32* was among the top 30 most highly induced on day 1.5 after infection (**Fig. 1b**). We confirmed the microarray data by quantitative reverse-transcription (qRT)-PCR, which revealed a >100-fold upregulation of the *Zbtb32* transcript in Ly49H$^+$ NK cells on day 2 after infection with MCMV (**Fig. 1c**), and by flow cytometry, which showed elevated Zbtb32 protein expression on days 2 and 3 after infection (**Supplementary Fig. 1**). Expression of *Zbtb32* transcript and protein were transient, and both returned to baseline abundance by day 4 after infection, which suggested an equally rapid downregulation of this transcription factor after its induction during viral infection.

Zbtb32 is required for NK cell antiviral immunity

Given its rapid upregulation after viral infection, we hypothesized that Zbtb32 might regulate the function and/or phenotype of activated antigen-specific NK cells. It has been shown previously that adoptively transferred Ly49H$^+$ NK cells can rescue NK cell–deficient or –impaired mice from otherwise fatal doses of MCMV[8]. To test the protective capacity of *Zbtb32*$^{-/-}$ NK cells, we transferred Ly49H$^+$ wild-type or Zbtb32-deficient NK cells into neonate mice, which lack mature B cells, T cells and NK cells and are highly susceptible to viral infection, and assessed the ability of the transferred cells to protect against lethal MCMV challenge[8,27]. As expected, wild-type Ly49H$^+$ NK cells had a significantly protective effect, with 33% of mice surviving past 3 weeks (median survival of 15 d; **Fig. 2a**). In contrast, neonates receiving *Zbtb32*$^{-/-}$ NK cells died early after infection (median survival of 8 d), similar to control animals that did not receive NK cells. To confirm the requirement for Zbtb32 in protective NK cell responses, we compared the ability of wild-type and *Zbtb32*$^{-/-}$ Ly49H$^+$ NK cells to protect adult Ly49H-deficient mice against lethal doses of recombinant vesicular stomatitis virus (VSV) expressing the MCMV-derived m157 protein (VSV-m157). In this model, mice infected with VSV-m157 rapidly succumb to paralysis and death in the absence of transferred Ly49H$^+$ NK cells. Whereas adoptively transferred wild-type Ly49H$^+$ NK cells protected ~50% of infected mice from death, all recipients of *Zbtb32*$^{-/-}$ Ly49H$^+$ NK cells died rapidly after infection, at a time comparable to animals that did not receive NK cells (**Fig. 2b**). Thus, Zbtb32 is required for protective antiviral responses by antigen-specific NK cells.

Zbtb32 is dispensable for NK cell activation and function

NK cells respond to MCMV infection by rapidly producing cytolytic proteins and proinflammatory cytokines, and for the subset of NK cells that express the Ly49H receptor, by proliferating to enlarge the overall pool of effector cells[1,7]. Given the protective defect of *Zbtb32*$^{-/-}$ NK cells, we sought to delineate which of these effector functions was controlled by Zbtb32. Zbtb32 has previously been shown to suppress cytokine production in activated T cells[28–32]. *Zbtb32*$^{-/-}$ CD4$^+$ T cells exhibited elevated expression of cytokines associated with type 2 helper T cells (T_H2 cells), including IL-4, IL-5 and IL-13, after activation *in vitro*[29] or in the context of allergen-induced models of airway and contact hypersensitivity *in vivo*[31,32]. Similarly, activated *Zbtb32*$^{-/-}$ CD8$^+$ T cells produced more IFN-γ than their wild-type counterparts[29]. In contrast to the findings in T cells, *Zbtb32*$^{-/-}$ and wild-type NK cells were indistinguishable in their ability to produce IFN-γ in response to MCMV infection *in vivo* (**Fig. 3a**), and after stimulation *in vitro* with proinflammatory cytokines or via cross-linking of activating receptors (**Supplementary Fig. 2a**). Furthermore, wild-type and *Zbtb32*$^{-/-}$ NK cells from MCMV-infected mice similarly upregulated expression of the potent cytotoxic protein granzyme B (**Fig. 3b**) and CD107a, a marker of degranulation (data not shown). In addition, NK cells in *Zbtb32*$^{-/-}$ mice were similar to those in wild-type animals with respect to their ability

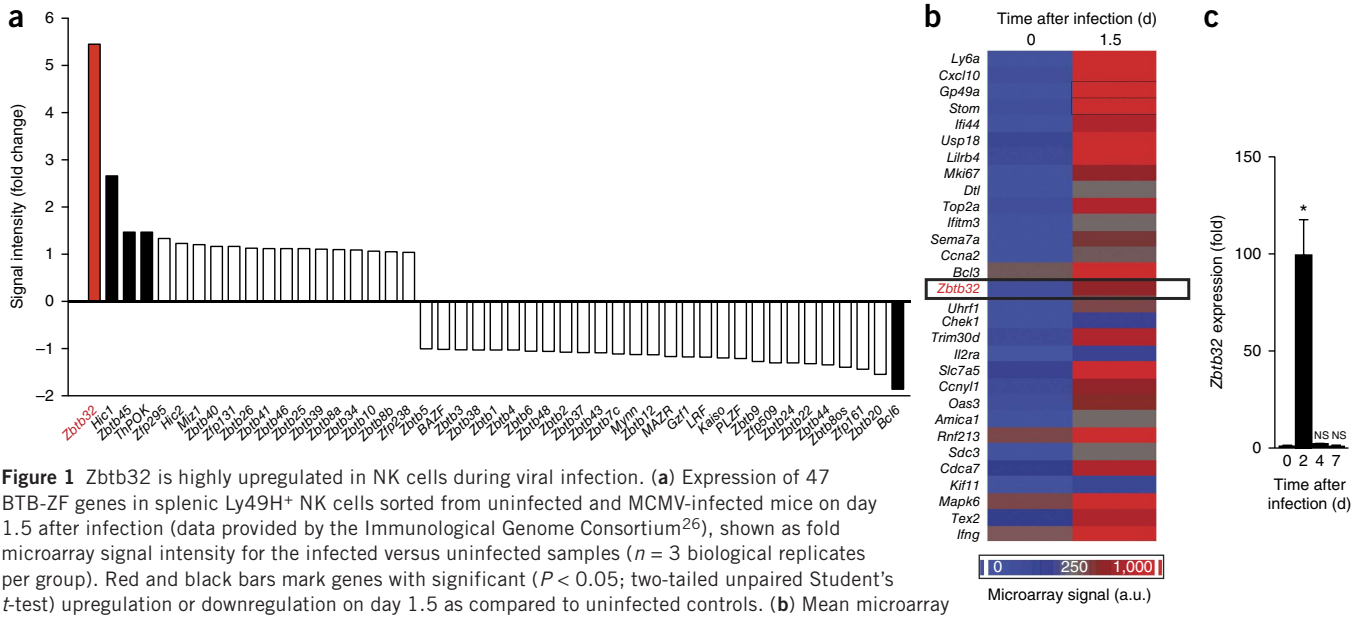

Figure 1 Zbtb32 is highly upregulated in NK cells during viral infection. (**a**) Expression of 47 BTB-ZF genes in splenic Ly49H$^+$ NK cells sorted from uninfected and MCMV-infected mice on day 1.5 after infection (data provided by the Immunological Genome Consortium[26]), shown as fold microarray signal intensity for the infected versus uninfected samples ($n = 3$ biological replicates per group). Red and black bars mark genes with significant ($P < 0.05$; two-tailed unpaired Student's *t*-test) upregulation or downregulation on day 1.5 as compared to uninfected controls. (**b**) Mean microarray signal intensity for top 30 most highly induced genes in splenic Ly49H$^+$ NK cells from MCMV-infected versus uninfected control mice ($n = 3$ biological replicates per time point). (**c**) qRT-PCR analysis of *Zbtb32* mRNA abundance in splenic Ly49H$^+$ NK cells sorted from MCMV-infected mice on days 2 ($n = 6$ mice), 4 ($n = 3$ mice) and 7 ($n = 3$ mice), shown as fold expression relative to uninfected mice ('day 0' in graph; $n = 5$ mice). Error bars, s.e.m. NS, not significant; $^*P < 0.05$ (two-tailed unpaired Student's *t*-test). Data show mean signal of $n = 3$ independent biological replicates from one experiment (**a**,**b**) and are representative of three independent experiments (**c**).

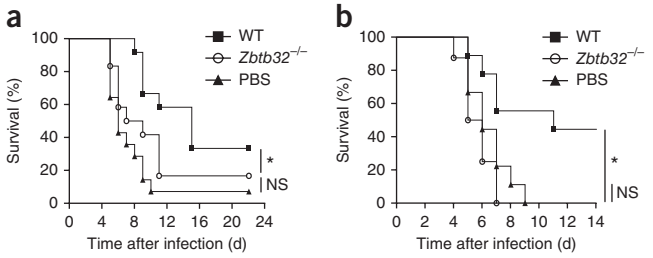

Figure 2 Zbtb32 is required for protective antiviral NK cell responses. (**a**) Kaplan-Meier survival curves for neonate Ly49H-deficient hosts receiving splenic Ly49H$^+$ NK cells from wild-type donors (WT; $n = 12$ mice) or *Zbtb32*$^{-/-}$ donors ($n = 12$ mice), or receiving phosphate-buffered saline (PBS) only ($n = 14$ mice), 1 d before infection with MCMV. (**b**) Kaplan-Meier survival curves for adult Ly49H-deficient hosts receiving splenic Ly49H$^+$ NK cells from WT ($n = 9$ mice) or *Zbtb32*$^{-/-}$ ($n = 8$ mice) donors, or receiving PBS only ($n = 9$ mice), 1 d before infection with VSV-m157. NS, not significant; $^*P < 0.05$ (Gehan-Breslow-Wilcoxon test). Data are pooled from four (**a**) and three (**b**) independent experiments.

to kill adoptively transferred target cells (**Supplementary Fig. 2b**). After MCMV infection, wild-type and *Zbtb32*$^{-/-}$ NK cells were comparable with respect to expression of the activation markers CD69 and KLRG1 (**Fig. 3c**), and both populations exhibited similar conversion to fully mature CD27^{lo}CD11b^{hi} cells by day 7 after infection (**Fig. 3d**). Taken together, our data indicate that the protective deficiency of *Zbtb32*$^{-/-}$ NK cells does not stem from a defect in killing capacity, cytokine production or maturation after viral infection.

Cell-intrinsic requirement for Zbtb32 in NK cell expansion

Given that effector responses were largely intact in Zbtb32-deficient NK cells, we postulated that their protective defect may arise from an impairment in antigen-driven proliferation. To test this hypothesis, we co-transferred equal numbers of *Zbtb32*$^{-/-}$ and wild-type Ly49H$^+$ NK cells into Ly49H-deficient hosts and evaluated the ability of the transferred Ly49H$^+$ cells to expand after MCMV infection (**Supplementary Fig. 3a**). Whereas the transferred wild-type Ly49H$^+$ NK cell population rapidly expanded and reached peak numbers and percentages in the spleen by day 7 after infection, transferred *Zbtb32*$^{-/-}$ Ly49H$^+$ NK cells were barely detectable at that time point (**Fig. 4a**,**b**). We obtained similar results when we transferred *Zbtb32*$^{-/-}$ and wild-type Ly49H$^+$ NK cells separately (**Fig. 4c**), which indicated that wild-type NK cells were not simply outcompeting their Zbtb32-deficient counterparts. The low numbers and percentages of *Zbtb32*$^{-/-}$ NK cells in the spleen were not due to aberrant trafficking, because we observed a similar deficiency in the liver, lymph node and lung (**Fig. 4d**). Moreover, the relative percentages of wild-type and *Zbtb32*$^{-/-}$ NK cells (~95% versus ~5%) remained constant from day 5 through day 45 after infection, ruling out delayed population expansion kinetics and a role for Zbtb32 in memory NK cell formation and maintenance (**Fig. 4e**). The requirement for Zbtb32 in antigen-specific NK cell expansion was not limited to MCMV infection, because the *Zbtb32*$^{-/-}$ Ly49H$^+$ NK cell population also exhibited an expansion defect after infection with m157-expressing VSV or m157-expressing VacV, although the magnitude of this defect was directly proportional to the number of cellular divisions driven by each virus (**Fig. 4f** and data not shown).

To test whether there exists a gene-dosage effect for Zbtb32 in antiviral NK cell responses, we individually co-transferred NK cells from *Zbtb32*$^{-/-}$, *Zbtb32*$^{+/-}$ or *Zbtb32*$^{+/+}$ littermates along with congenic wild-type NK cells into Ly49H-deficient hosts. As expected, the Ly49H$^+$ NK cell population from *Zbtb32*$^{+/+}$ mice expanded as well as that from wild-type donors, whereas the Ly49H$^+$ NK cell population from *Zbtb32*$^{-/-}$ littermates barely expanded at all, which confirmed that Zbtb32 deficiency, and not background-related effects, was responsible for the expansion defect (**Fig. 4g**). To our surprise, Ly49H$^+$ NK cells containing only one *Zbtb32* allele (*Zbtb32*$^{+/-}$) were almost as dysfunctional as fully deficient *Zbtb32*$^{-/-}$ NK cells, which underscored that maximal Zbtb32 expression is required for expansion of the NK cell population after infection.

Because Zbtb32 is also upregulated in antigen-specific CD8$^+$ T cells after viral or bacterial infection (data not shown), and has previously been reported to regulate T cell proliferation *in vitro* (although these studies suggested a restrictive role for Zbtb32 in TCR-driven proliferation)[29,33], we measured the expansion of antigen-specific CD8$^+$ T cells in wild-type:*Zbtb32*$^{-/-}$ mixed bone marrow chimeras during MCMV infection (**Fig. 4h**). In contrast to our findings in NK cells, Zbtb32-deficient antigen-specific CD8$^+$ T cell populations expanded similarly or better than their wild-type counterparts. Thus, taken together, our data indicate an essential cell-intrinsic and lineage-specific function for Zbtb32 in promoting NK cell expansion after infection.

Zbtb32 controls NK cell proliferation but not survival

We next investigated the extent to which Zbtb32 controlled the various cellular processes of proliferation, survival and apoptosis in activated NK cells, any one of which could explain the observed population expansion defect. Transfer of Ly49H$^+$ NK cells labeled

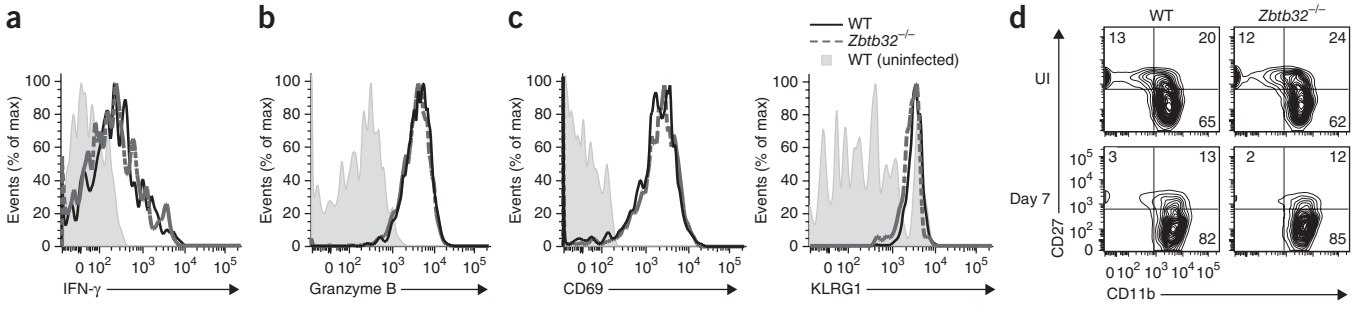

Figure 3 Zbtb32 is dispensable for NK cell activation, maturation and expression of effector molecules. (**a**,**b**) Intracellular IFN-γ (**a**) and intracellular granzyme B (**b**) in splenic wild-type (WT) or *Zbtb32*$^{-/-}$ Ly49H$^+$ NK cells from mixed bone marrow chimeric mice on day 2 after infection with MCMV. (**c**) CD69 and KLRG1 expression on transferred WT and *Zbtb32*$^{-/-}$ Ly49H$^+$ NK cells in the spleen on day 2 (for CD69) or day 7 (for KLRG1) after infection with MCMV. Ly49H$^+$ NK cell populations were co-transferred into recipient Ly49H-deficient mice 1 d before infection. (**d**) Percentage of immature (CD27^{hi}CD11b^{lo} and CD27^{hi}CD11b^{hi}) and mature (CD27^{lo}CD11b^{hi}) Ly49H$^+$ NK cells in the spleen of uninfected (UI) or MCMV-infected (day 7 after infection) mixed bone marrow chimeric animals. Numbers in quadrants show the percentage of cells in each quadrant. Data are representative of $n = 5$ (infected) and $n = 2$ (uninfected) mice (**a**,**b**), of $n = 5$ mice per time point (**c**), and $n = 7$ (infected) and $n = 2$ (uninfected) mice (**d**) from two independent experiments.

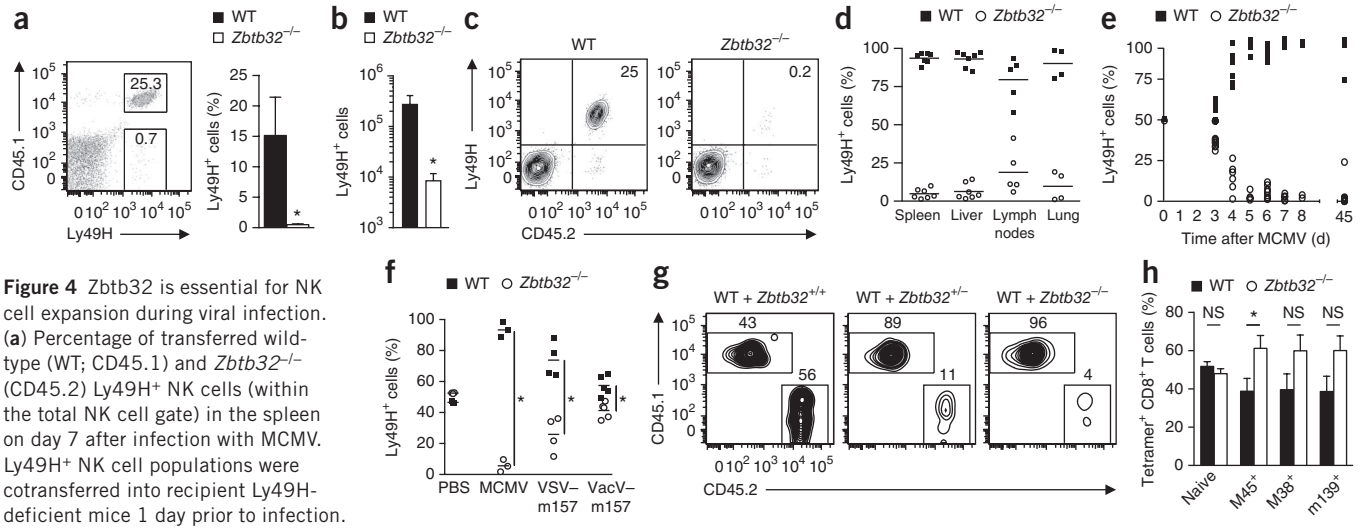

Figure 4 Zbtb32 is essential for NK cell expansion during viral infection. (**a**) Percentage of transferred wild-type (WT; CD45.1) and *Zbtb32*$^{-/-}$ (CD45.2) Ly49H^{+} NK cells (within the total NK cell gate) in the spleen on day 7 after infection with MCMV. Ly49H^{+} NK cell populations were cotransferred into recipient Ly49H-deficient mice 1 day prior to infection. Numbers in plots indicate percentage of cells in the gates. $^{*}P < 0.05$ in a ratio-paired two-tailed *t*-test. (**b**) As in **a**, except showing absolute number. $^{*}P < 0.05$, ratio-paired two-tailed *t*-test. (**c**) Percentage of transferred WT or *Zbtb32*$^{-/-}$ Ly49H^{+} NK cells (among total NK cells) in the spleen on day 7 after infection with MCMV, where each Ly49H^{+} NK cell population was separately transferred into independent recipient Ly49H-deficient mice (CD45.1^{+}) 1 day prior to infection. (**d**) Relative percentages of transferred WT and *Zbtb32*$^{-/-}$ Ly49H^{+} NK cells in various organs on day 7 after infection with MCMV. Ly49H^{+} NK cell populations were co-transferred into recipient Ly49H-deficient mice 1 d before infection. Symbols represent individual mice. (**e**) As in **d**, except in the spleen at specified time points after infection with MCMV. (**f**) As in **d**, except in the spleen on day 8 after infection with the indicated viruses. (**g**) As in **d**, except the *Zbtb32* NK cells were from *Zbtb32*$^{-/-}$, *Zbtb32*$^{+/-}$ or *Zbtb32*$^{+/+}$ littermates. Plots show co-transferred WT (CD45.1) and *Zbtb32* (CD45.2) Ly49H^{+} NK cells in the spleen on day 7 after infection. Numbers in plots indicate percentage of cells in the gates. (**h**) Relative percentage of WT and *Zbtb32*$^{-/-}$ tetramer^{+} CD8^{+} T cells in WT:*Zbtb32*$^{-/-}$ mixed bone marrow chimeric mice on day 7 (for M45^{+}) or day 14 (for m139^{+} or M38^{+}) after infection with MCMV ($n = 8$ animals). NS, not significant; $^{*}P < 0.05$ (two-tailed unpaired Student's *t*-test). Data on the left are representative of and graph on right shows mean + s.e.m. for $n = 3$ mice (**a**). Data are representative of four independent experiments (**a**), representative of two independent experiments (**b**), representative of $n = 4$ mice per group from two independent experiments (**c**), cumulative from three independent experiments (**d**), cumulative for five independent experiments, $n = 10$ (day 3), $n = 6$ (day 4), $n = 4$ (day 5), $n = 8$ (day 6), $n = 5$ (day 7), $n = 2$ (day 8) and $n = 9$ (day 45) (**e**), representative of at least two independent experiments (**f**), representative of $n = 3$ mice per group in each of two independent experiments (**g**), and representative of three independent experiments (**h**). All error bars, s.e.m.

with division-tracking dye CFSE confirmed that Zbtb32 deficiency markedly impaired MCMV-driven proliferation *in vivo* (**Fig. 5a**). The impaired proliferative capacity of *Zbtb32*$^{-/-}$ Ly49H^{+} NK cells was corroborated by their decreased expression of the proliferation marker Ki67 (**Fig. 5b**) and by their inability to incorporate 5-bromodeoxyuridine (BrdU) after short-term pulses on days 4 and 6 after infection (**Fig. 5c**). This defect was mirrored at a molecular level by a failure of Zbtb32-deficient NK cells to upregulate genes involved in cell-cycle progression (**Fig. 5d**).

Because Zbtb32 was upregulated to a similar extent in both Ly49H^{+} and Ly49H^{-} NK cells after infection (**Supplementary Fig. 3b**), we tested whether Zbtb32 might also regulate the low-level NK cell proliferation that occurs independently of Ly49H-m157 engagement. Indeed, even Ly49H^{-} NK cells showed impaired proliferation in the absence of Zbtb32, as did Ly49H^{+} NK cells responding to infection with MCMV Δm157 (**Supplementary Fig. 3c**,**d**), although this defect was subtle given that all NK cells proliferated very little in these settings.

In contrast to their proliferation defect, *Zbtb32*$^{-/-}$ NK cells exhibited no evidence of enhanced apoptosis by staining for annexin V, the proapoptotic molecule Bim or activated caspases (**Fig. 5e** and data not shown). In T cells, the prosurvival protein Bcl-2 is downregulated in effector cells with the highest proliferative capacity, and subsequent apoptosis of these highly proliferative Bcl-2^{lo} cells marks the contraction phase of the effector T cell response[34,35]. Consistent with a defect in proliferation but not survival, *Zbtb32*$^{-/-}$ NK cells failed to undergo activation-induced downregulation of Bcl-2 (**Fig. 5f**). Thus, these findings highlight a specific requirement for Zbtb32 in the proliferation but not survival of NK cells after viral infection.

Zbtb32 is dispensable for development and homeostasis

The NK cell compartment of *Zbtb32*$^{-/-}$ mice was phenotypically indistinguishable from that of wild-type animals, which suggested that Zbtb32 deficiency neither impaired development of NK cells nor abrogated proliferation in that context. The percentage and number of mature NK cells in peripheral organs and of NK cell developmental subsets in the bone marrow of Zbtb32-deficient mice was comparable to that observed in wild-type animals (**Supplementary Fig. 4a**,**b** and data not shown). Similarly, NK cells in *Zbtb32*$^{-/-}$ mice expressed normal amounts of markers typically associated with NK cell identity and function, including Ly49H, Ly49D, NK1.1, DX5, Ly49C or Ly49I and Ly49A (**Supplementary Fig. 4c**,**d**).

In addition, wild-type and Zbtb32-deficient NK cells repopulated the hematopoietic compartment of mixed bone marrow chimeric mice with similar efficiencies (**Supplementary Fig. 5**), confirming that Zbtb32 was dispensable for NK cell development. However, when we adoptively transferred wild-type and *Zbtb32*$^{-/-}$ Ly49H^{+} NK cells from mixed bone marrow chimeric mice into naive Ly49H-deficient recipients, only the wild-type population expanded after MCMV challenge, which reaffirmed that even *Zbtb32*$^{-/-}$ NK cells that developed in a Zbtb32-sufficient environment exhibited an expansion defect after infection (**Supplementary Fig. 5**). Consistent with a dispensable role in NK cell proliferation during development, *Zbtb32*$^{-/-}$ NK cells exhibited normal homeostatic proliferation when transferred into lymphocyte-deficient hosts (**Fig. 5g**) and when expanded *ex vivo* with IL-2 and IL-15, cytokines important for proliferation and survival of NK cells during development and at steady state (**Fig. 5h**). Thus, Zbtb32 does not appear to be necessary for NK cell proliferation in a noninflammatory environment. Collectively, our data indicate that Zbtb32 is dispensable for development and

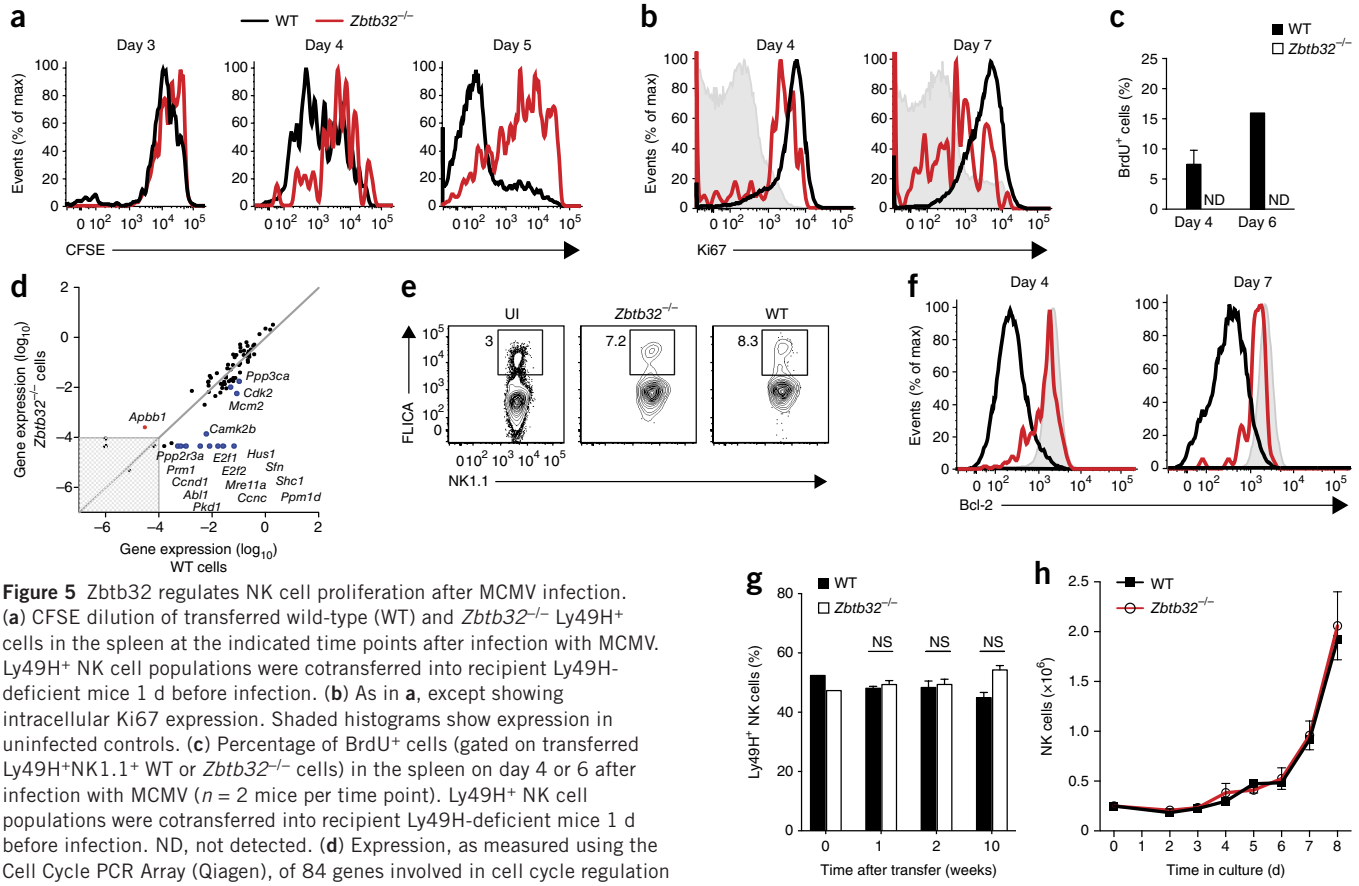

Figure 5 Zbtb32 regulates NK cell proliferation after MCMV infection. (**a**) CFSE dilution of transferred wild-type (WT) and *Zbtb32*$^{-/-}$ Ly49H^{+} cells in the spleen at the indicated time points after infection with MCMV. Ly49H^{+} NK cell populations were cotransferred into recipient Ly49H-deficient mice 1 d before infection. (**b**) As in **a**, except showing intracellular Ki67 expression. Shaded histograms show expression in uninfected controls. (**c**) Percentage of BrdU^{+} cells (gated on transferred Ly49H^{+}NK1.1^{+} WT or *Zbtb32*$^{-/-}$ cells) in the spleen on day 4 or 6 after infection with MCMV ($n = 2$ mice per time point). Ly49H^{+} NK cell populations were cotransferred into recipient Ly49H-deficient mice 1 d before infection. ND, not detected. (**d**) Expression, as measured using the Cell Cycle PCR Array (Qiagen), of 84 genes involved in cell cycle regulation in sorted WT and *Zbtb32*$^{-/-}$Ly49H^{+} NK cells on day 4 after infection with MCMV. Ly49H^{+} NK cell populations were cotransferred into recipient Ly49H-deficient mice 1 d before infection. Genes upregulated (red) or downregulated (blue) >fourfold in *Zbtb32*$^{-/-}$ versus WT Ly49H^{+} splenic NK cells are annotated. Gray shading shows limit of detection for the assay. (**e**) Percentage of FLICA^{+} cells (gated on transferred Ly49H^{+}NK1.1^{+} WT or *Zbtb32*$^{-/-}$ cells) in the spleen on day 4 after infection with MCMV or in WT uninfected (UI) mice. Ly49H^{+} NK cell populations were cotransferred into recipient Ly49H-deficient mice 1 d before infection. Numbers in plots indicate percentage of FLICA^{+} cells in gates. (**f**) As in **b**, except showing intracellular Bcl-2 expression. (**g**) Relative percentages of co-transferred WT and *Zbtb32*$^{-/-}$ Ly49H^{+} NK cells in the peripheral blood (0, 1 and 2 weeks) or spleen (10 weeks) of *Rag2*$^{-/-}$*Il2rg*$^{-/-}$ recipients at the indicated time points after transfer. NS, not significant (two-tailed unpaired Student's *t*-test). (**h**) Absolute number of WT and *Zbtb32*$^{-/-}$ NK cells after incubation *ex vivo* with IL-2 and IL-15 for the indicated number of days. Data are representative of $n = 6$ mice per time point from three independent experiments (**a**), representative of $n = 4$ mice per time point from two independent experiments (**b**), representative of two independent experiments (**c**), representative of one experiment ($n = 5$ mice pooled) (**d**), representative of $n = 2$ mice per group in each of two independent experiments (**e**), representative of $n = 2$ mice per group in each of three independent experiments (**f**) show mean of $n = 3$ mice per time point in each of 2 independent experiments (**g**), and representative of $n = 3$ biological replicates per group from two independent experiments (**h**). All error bars, s.e.m.

homeostasis-associated proliferation but rather specifically regulates proliferation of NK cells in the context of an infectious or inflammatory setting.

Inflammation drives Zbtb32 expression in NK cells

Because we observed maximal levels of *Zbtb32* mRNA in NK cells at early time points *in vivo* (by ~48 h after infection), when inflammation is high but viral dissemination (and thus antigen availability) is still lagging, and because both Ly49H^{+} and Ly49H^{-} NK cells upregulated Zbtb32 after infection, we hypothesized that signals from proinflammatory cytokines, rather than interactions between the Ly49H receptor and the m157 viral antigen, might control *Zbtb32* expression in activated NK cells. Indeed, in resting NK cells stimulated *ex vivo*, the proinflammatory cytokines IL-12, IL-18 or IFN-α/β induced high expression of *Zbtb32* mRNA, with IL-12 and IL-18 cotreatment exerting a strongly synergistic effect (**Fig. 6a**). In contrast, *Zbtb32* mRNA was barely detectable after cross-linking of the activating receptors Ly49H, Ly49D, NKG2D or NKp46. To test whether signals from proinflammatory cytokines were required for *Zbtb32* induction *in vivo*, we used mixed bone marrow chimeric mice harboring both wild-type NK cells and NK cells lacking receptors for either type I interferons, IL-12 or IL-18, or for both type I interferons and IL-12. Compared to their wild-type counterparts, cytokine receptor–deficient NK cells were markedly impaired in their ability to upregulate *Zbtb32* mRNA after MCMV infection *in vivo*, with NK cells lacking both the IL-12 and the type I interferon receptors showing the greatest defect (**Fig. 6b**).

Given that proinflammatory cytokines induce *Zbtb32*, we postulated that specific transcriptional activators downstream of cytokine receptors might directly regulate *Zbtb32* expression in NK cells. Analysis of the *Zbtb32* promoter revealed several conserved noncoding sites (CNSs) in a DNase I hypersensitivity region previously identified in human NK cells[36] (**Fig. 6c**). Chromatin immunoprecipitation (ChIP) experiments showed enrichment of acetylated histone marks at these sites (specifically, H3K27Ac, which marks transcriptionally active promoters), consistent with a likely role in transcriptional activation of *Zbtb32* (**Fig. 6d**). In support of direct regulation by cytokine receptor signaling, the CNS regions of the *Zbtb32* promoter harbor putative binding sites for the transcription factor STAT4, which acts downstream of the IL-12 receptor to induce target gene expression in lymphocytes (**Fig. 6c**). Similar to the case in IL-12R–deficient NK cells, NK cells lacking STAT4 were also significantly impaired

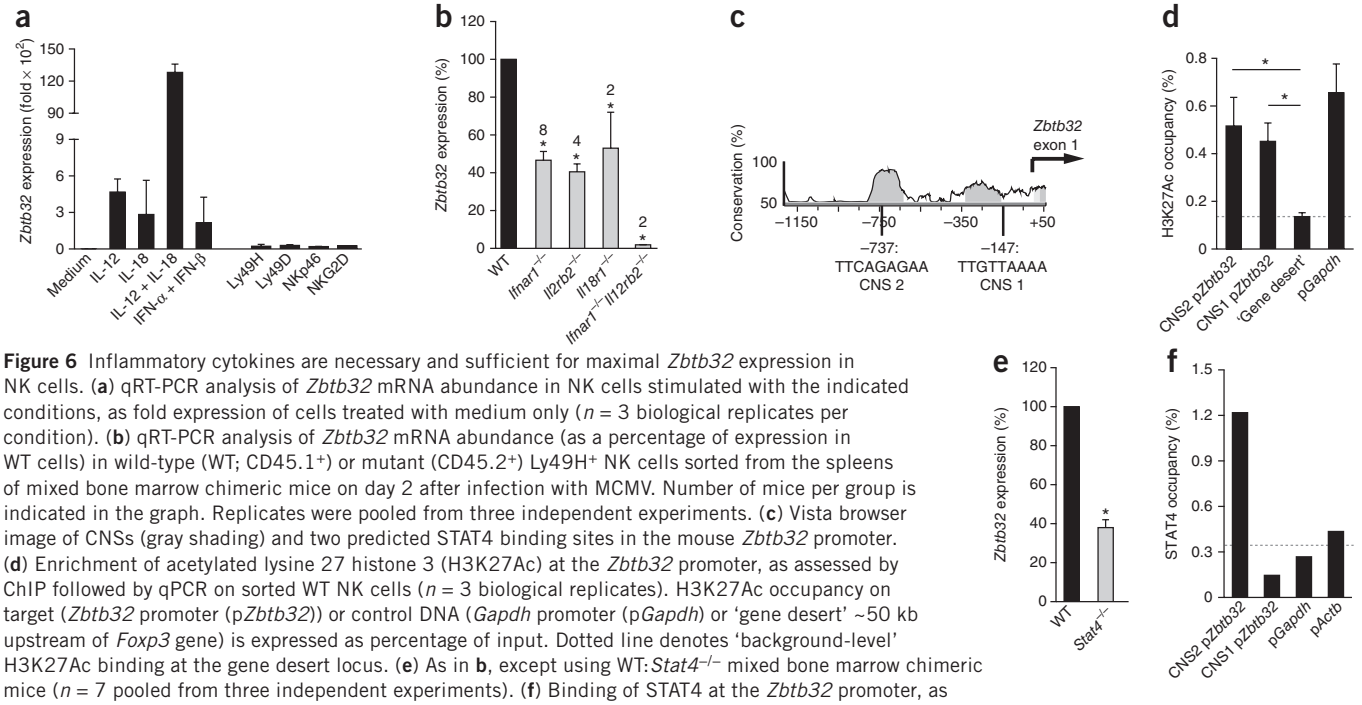

Figure 6 Inflammatory cytokines are necessary and sufficient for maximal *Zbtb32* expression in NK cells. (**a**) qRT-PCR analysis of *Zbtb32* mRNA abundance in NK cells stimulated with the indicated conditions, as fold expression of cells treated with medium only ($n = 3$ biological replicates per condition). (**b**) qRT-PCR analysis of *Zbtb32* mRNA abundance (as a percentage of expression in WT cells) in wild-type (WT; CD45.1$^+$) or mutant (CD45.2$^+$) Ly49H$^+$ NK cells sorted from the spleens of mixed bone marrow chimeric mice on day 2 after infection with MCMV. Number of mice per group is indicated in the graph. Replicates were pooled from three independent experiments. (**c**) Vista browser image of CNSs (gray shading) and two predicted STAT4 binding sites in the mouse *Zbtb32* promoter. (**d**) Enrichment of acetylated lysine 27 histone 3 (H3K27Ac) at the *Zbtb32* promoter, as assessed by ChIP followed by qPCR on sorted WT NK cells ($n = 3$ biological replicates). H3K27Ac occupancy on target (*Zbtb32* promoter (p*Zbtb32*)) or control DNA (*Gapdh* promoter (p*Gapdh*) or 'gene desert' ~50 kb upstream of *Foxp3* gene) is expressed as percentage of input. Dotted line denotes 'background-level' H3K27Ac binding at the gene desert locus. (**e**) As in **b**, except using WT:*Stat4*$^{-/-}$ mixed bone marrow chimeric mice ($n = 7$ pooled from three independent experiments). (**f**) Binding of STAT4 at the *Zbtb32* promoter, as assessed by ChIP followed by qPCR, in sorted WT NK cells stimulated for 24 h with IL-12 and IL-18. STAT4 occupancy of target (p*Zbtb32*) or control (p*Actb* and p*Gapdh*) promoter DNA is expressed as a percentage of input. Dotted line denotes 'background-level' STAT4 binding, set as the mean STAT4 binding of control promoter DNA. Data are representative of three independent experiments (**a**,**d**) and representative of $n = 3$ mice (pooled) in each of two independent experiments (**f**). *$P < 0.05$ (two-tailed unpaired Student's *t*-test). All error bars, s.e.m.

in MCMV-induced *Zbtb32* expression (**Fig. 6e**). Using STAT4 ChIP, we observed substantial binding of STAT4 at a CNS in the *Zbtb32* promoter ~750 base pairs upstream of the transcriptional start site, which indicated that *Zbtb32* may be a direct target of STAT4, acting as a transmitter of IL-12 signaling (**Fig. 6f**). Decreased *Zbtb32* expression correlates with the impaired proliferation recently observed in IL-12R– or STAT4-deficient NK cells[37], consistent with a central role for Zbtb32 in transmitting proproliferative signals downstream of inflammatory cues. Thus, signals from proinflammatory cytokines, but not activating receptors, are sufficient to induce and are required for maximal *Zbtb32* expression in primary NK cells.

Zbtb32 promotes proliferation by antagonizing Blimp-1

We next sought to identify the specific pathway(s) regulated by Zbtb32 in proliferating NK cells. Zbtb32 deficiency did not affect expression or phosphorylation of STAT1, STAT3, STAT4 or T-bet in activated NK cells, transcription factors with proven or suspected roles in NK cell effector function[37–39], nor did it influence expression of *Gata3*, a known target of Zbtb32 in T cells[28,30] (**Supplementary Fig. 6a**). These data are consistent with our findings that the nonproliferative features of NK cell activation, including production of IFN-γ and cytotoxic molecules, are intact in the absence of Zbtb32.

Because cell-cycle genes are dysregulated in *Zbtb32*$^{-/-}$ NK cells during MCMV infection (**Fig. 5d**), we investigated the mechanism(s) by which Zbtb32 may promote cell-cycle progression in NK cells. In T cells and B cells, proliferation of effector lymphocytes (for example, germinal center B cells) depends on suppression of the antiproliferative/proterminal differentiation factor, Blimp-1 (encoded by *Prdm1*)[40]. Blimp-1 is upregulated in NK cells during development, where it functions to restrict proliferation, and remains highly expressed in mature resting NK cells. Although the BTB-ZF protein Bcl-6 is the main antagonist of Blimp-1 in B cells and T cells[40], it does not have this role

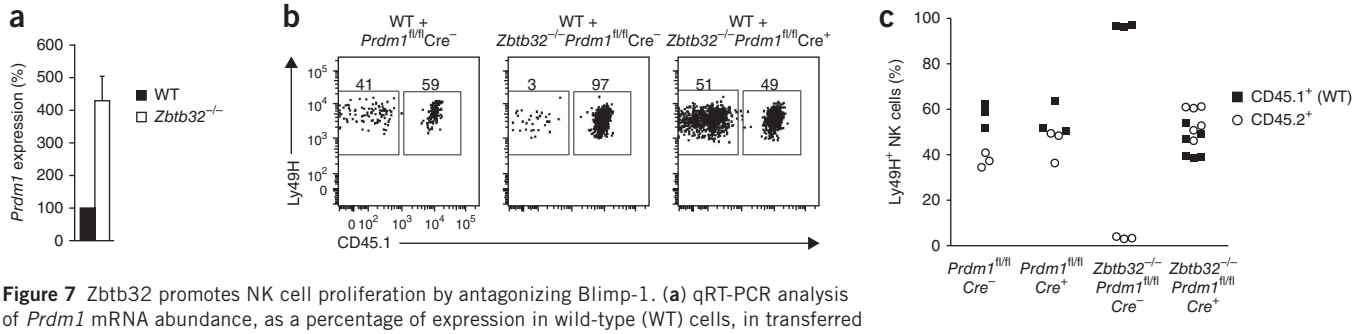

Figure 7 Zbtb32 promotes NK cell proliferation by antagonizing Blimp-1. (**a**) qRT-PCR analysis of *Prdm1* mRNA abundance, as a percentage of expression in wild-type (WT) cells, in transferred WT and *Zbtb32*$^{-/-}$ Ly49H$^+$ NK cells sorted from the spleen on day 4 after infection with MCMV ($n = 4$ mice). The Ly49H$^+$ NK cell populations were cotransferred into recipient Ly49H-deficient mice 1 d before infection. Error bars, s.e.m. (**b**,**c**) Relative percentages of transferred WT (CD45.1) and littermate (CD45.2) Ly49H$^+$ NK cells in the spleen on day 7 after infection with MCMV. Ly49H$^+$ NK cell populations were cotransferred into recipient Ly49H-deficient mice 1 d before infection. CD45.2$^+$ NK cells are from *Prdm1*$^{fl/fl}$*Nkp46-Cre*$^-$, *Prdm1*$^{fl/fl}$*Nkp46-Cre*$^+$, *Zbtb32*$^{-/-}$*Prdm1*$^{fl/fl}$*Nkp46-Cre*$^-$ or *Zbtb32*$^{-/-}$*Prdm1*$^{fl/fl}$*Nkp46-Cre*$^+$ littermates. Shown are representative responses in individual mice (**b**; except the WT + *Prdm1*$^{fl/fl}$*Nkp46-Cre*$^+$ cohort) and summary data (**c**), where each symbol represents an individual mouse. Data are representative of two (**a**) and three (**b**,**c**) independent experiments.

in developing NK cells[41] and is unlikely to do so in activated NK cells, because Bcl-6 is actually downregulated after infection (**Fig. 1b** and **Supplementary Fig. 6b**). Given the high degree of homology between Bcl-6 and Zbtb32, we hypothesized that Zbtb32 rather than Bcl-6 may function in activated NK cells to suppress expression or function of Blimp-1 and thereby facilitate antigen-driven proliferation. This idea was supported by a recent report that showed a physical interaction between Zbtb32 and Blimp-1 in B cells[42] and our own observation that *Prdm1* expression was elevated in *Zbtb32*$^{-/-}$ Ly49H^{+} NK cells (**Fig. 7a**). However, to formally test this hypothesis, we generated mice harboring NK cells in which both *Zbtb32* and *Prdm1* were genetically deleted, by crossing *Zbtb32*$^{-/-}$ mice to mice carrying *Prdm1* alleles flanked by *lox*P sites (*Prdm1*$^{fl/fl}$) and mice containing the Cre recombinase driven from the *NKp46* promoter (*Nkp46-Cre*$^{+}$). We predicted that if the primary function of Zbtb32 was to suppress or antagonize Blimp-1 function, then deletion of Blimp-1 in Zbtb32-deficient NK cells should result in a partial or complete restoration of Ly49H^{+} NK cell expansion during MCMV infection. Indeed, we found that whereas NK cells from *Zbtb32*$^{-/-}$*Prdm1*$^{fl/fl}$*Nkp46-Cre*$^{-}$ (Zbtb32-deficient only) donors were severely impaired in their ability to expand after infection, NK cells from *Zbtb32*$^{-/-}$*Prdm1*$^{fl/fl}$*Nkp46-Cre*$^{+}$ (Zbtb32 and Blimp-1 double-deficient) littermates were fully rescued from this defect and proliferated as well as wild-type cells (**Fig. 7b**,**c**). Thus, consistent with our hypothesis, Zbtb32 was no longer required for MCMV-driven NK cell proliferation when Blimp-1 was not present. These findings provide a molecular explanation for how Zbtb32 acts downstream of proinflammatory signals to promote a proproliferative state in activated NK cells, and reveal an antagonistic interaction between Zbtb32 and Blimp-1 that regulates NK cell expansion during infection (**Supplementary Fig. 7**).

DISCUSSION

A growing number of recent studies in mice and humans have led to the unexpected discovery that NK cells can mount antigen-specific responses with features of adaptive immunity, including robust clonal proliferation, long-term persistence and enhanced secondary responses of virus-specific NK cells[1]. Before now, the molecular events that regulate these antigen-specific responses were almost completely unknown. Here we demonstrated that the transcription factor Zbtb32 is essential for the proliferation and protective functionality of MCMV-specific NK cells responding to infection. Zbtb32 deficiency ablated the proliferative burst of antigen-specific NK cells and impaired the low-level proliferation driven by antigen-independent signals in 'bystander' NK cells. We also showed that signals from proinflammatory cytokines were necessary and sufficient to induce *Zbtb32* expression in activated NK cells. At a mechanistic level, Zbtb32 promoted a proproliferative state in activated NK cells by antagonizing the tumor suppressor factor, Blimp-1. In summary, in this study we elucidated the molecular pathway behind the proliferative burst of antigen-specific NK cells and demonstrated not only that Zbtb32 is the molecular 'link' between inflammation and proliferation in NK cells but also revealed a previously uncharacterized antagonistic interaction between Zbtb32 and Blimp-1.

The finding that proinflammatory cytokines are essential for maximal *Zbtb32* expression provides a mechanistic explanation for how and why inflammatory signals are required for the robust proliferation of antigen-specific NK cells during MCMV infection, even when high amounts of viral antigen are available[37]. This pathway may be analogous to 'signal 3' in the widely accepted model of T cell activation, which holds that full effector function relies on three independent and cotemporal signals from the TCR (signal 1), co-stimulatory receptors such as CD28 (signal 2), and cytokine receptors such as IFNAR and IL-12R (signal 3). In a similar manner, inflammation-driven upregulation of Zbtb32 may act as an important checkpoint for effector responses by NK cells, only allowing robust antigen-driven proliferation when clear signals of infection are present. Indeed, the intimate connection between inflammation and Zbtb32 expression is consistent with our finding that Zbtb32 is dispensable for NK cell proliferation in noninflammatory settings, such as during development, homeostatic turnover and long-term maintenance of memory cells.

During infection, both IL-12 signaling (for example, as reflected by STAT4 phosphorylation) and Zbtb32 expression peak early after infection, yet this pathway has a critical, long-lasting impact on the proliferative response that continues for days after these initiating signals have returned to baseline. These findings are consistent with a model in which Zbtb32 acts as a 'priming' signal in inflammation-activated NK cells, suppressing Blimp-1 function and thereby unleashing a long-lasting proliferative potential in antigen-specific and nonspecific NK cells responding to infection. We speculate that this may be achieved, at least in part, by the well-established function of both Blimp-1 and BTB-ZF proteins (including Zbtb32) in remodeling the chromatin environment at target loci by recruiting histone modifying enzymes, including histone acetylases, histone methyltransferases and histone deacetylases[10,43,44]. Perhaps Zbtb32 promotes proliferation in NK cells by suppressing or subverting the ability of Blimp-1 to alter chromatin structure at certain loci such as proproliferative and antiproliferative target genes, and in this way permits the proliferative responses that continue for days after Zbtb32 expression peaks. In support of this idea, a recent study in B cells demonstrated that Zbtb32 and Blimp-1 could physically interact at a protein level and could colocalize at certain loci targeted by Blimp-1 (ref. 42). It will be interesting to determine whether Zbtb32 also complexes with Blimp-1 in NK cells, and whether such an interaction might explain the antagonistic relationship between Zbtb32 and Blimp-1 in NK cell proliferation.

The role of Zbtb32 in regulating tumor suppressor and cell cycle pathways in NK cells is consistent with the reported functions of other BTB-ZF family members, both in lymphocytes and in nonhematopoietic cells[9,10]. For example, LRF has been shown to repress *Cdkn1a* (also known as *p21*) and *Cdkn2a* (also known as *p19Arf*) in germinal center B cells[45]. Similarly, Bcl-6 facilitates the survival and proliferation of germinal center B cells undergoing class switch recombination and somatic hypermutation by repressing transcription of the tumor suppressor genes *TP53* and *Prdm1*, and the cell-cycle arrest gene *CDNK1A* (refs. 40,46–49). Our finding that Zbtb32 regulates NK cell proliferation principally by antagonizing Blimp-1 sheds light on the previously unexplained observation that NK cells could robustly proliferate during infection despite expressing consistently high amounts of Blimp-1 (ref. 41), a factor generally recognized to restrain lymphocyte proliferation[40].

Similar to our findings in MCMV-infected mice, recent studies have described clonal-like NK cell proliferation and long-lived memory-like NK cells in humans infected with human CMV[50–52]. In as much as proinflammatory cytokines can drive certain adaptive immune properties in human NK cells *in vitro*[53], it will be important to determine whether the human Zbtb32 homolog also controls antigen-specific NK cell responses in humans during pathogen infection. Nonetheless, our current findings uncover previously unidentified molecular events that control antigen-specific NK cell responses and may have potential utility in informing therapeutic approaches that harness NK cells in the treatment of human disease.

METHODS

Methods and any associated references are available in the online version of the paper.

Accession codes. Gene expression omnibus: GSE15907.

Note: Any Supplementary Information and Source Data files are available in the online version of the paper.

ACKNOWLEDGMENTS

We thank members of the Sun lab for technical support and experimental assistance, members of the Memorial Sloan-Kettering NK club for insightful comments and helpful discussions, A. Rudensky, M. van den Brink, M. Li, L. Lanier (University of California San Francisco), D. Sant'Angelo (Rutgers University) and L. Denzin (Rutgers University) for sharing antibodies and flow cytometry resources and for providing expertise critical to this study and manuscript, G. Gasteiger, K. Schluns (M.D. Anderson) and U. Koszinowski (Max von Pettenkofer-Institute) for providing many of the parent and recombinant viruses used in our study, S. Way (University of Minnesota) for providing femurs from *Il12rb2*$^{-/-}$ × *Ifnar1*$^{-/-}$ mice for use in making bone marrow chimeras, the Immunological Genome Consortium for providing the microarray data used in this study[26], and J.P. Houchins and his team at R&D Systems for providing the experimental anti-Zbtb32 flow cytometry antibody used in this study. A.M.B. was supported by US National Institutes of Health T32 award (CA009149). J.C.S. was supported by the Searle Scholars Program, the Cancer Research Institute, and grants from the National Institutes of Health (AI085034 and AI100874).

AUTHOR CONTRIBUTIONS

A.M.B. and C.L.Z. performed the experiments; T.N. provided the *Zbtb32*$^{-/-}$ mice and feedback on the manuscript; A.M.B. and J.C.S. designed the study and wrote the manuscript.

COMPETING FINANCIAL INTERESTS

The authors declare no competing financial interests.

1. Sun, J.C. & Lanier, L.L. NK cell development, homeostasis and function: parallels with CD8(+) T cells. *Nat. Rev. Immunol.* **11**, 645–657 (2011).
2. Smith, H.R. *et al.* Recognition of a virus-encoded ligand by a natural killer cell activation receptor. *Proc. Natl. Acad. Sci. USA* **99**, 8826–8831 (2002).
3. Arase, H., Mocarski, E.S., Campbell, A.E., Hill, A.B. & Lanier, L.L. Direct recognition of cytomegalovirus by activating and inhibitory NK cell receptors. *Science* **296**, 1323–1326 (2002).
4. Daniels, K.A. *et al.* Murine cytomegalovirus is regulated by a discrete subset of natural killer cells reactive with monoclonal antibody to Ly49H. *J. Exp. Med.* **194**, 29–44 (2001).
5. Brown, M.G. *et al.* Vital involvement of a natural killer cell activation receptor in resistance to viral infection. *Science* **292**, 934–937 (2001).
6. Bubic, I. *et al.* Gain of virulence caused by loss of a gene in murine cytomegalovirus. *J. Virol.* **78**, 7536–7544 (2004).
7. Dokun, A.O. *et al.* Specific and nonspecific NK cell activation during virus infection. *Nat. Immunol.* **2**, 951–956 (2001).
8. Sun, J.C., Beilke, J.N. & Lanier, L.L. Adaptive immune features of natural killer cells. *Nature* **457**, 557–561 (2009).
9. Kelly, K.F. & Daniel, J.M. POZ for effect–POZ-ZF transcription factors in cancer and development. *Trends Cell Biol.* **16**, 578–587 (2006).
10. Beaulieu, A.M. & Sant'Angelo, D.B. The BTB-ZF family of transcription factors: key regulators of lineage commitment and effector function development in the immune system. *J. Immunol.* **187**, 2841–2847 (2011).
11. Maeda, T. *et al.* Regulation of B versus T lymphoid lineage fate decision by the proto-oncogene LRF. *Science* **316**, 860–866 (2007).
12. Bilic, I. *et al.* Negative regulation of CD8 expression via Cd8 enhancer-mediated recruitment of the zinc finger protein MAZR. *Nat. Immunol.* **7**, 392–400 (2006).
13. Sakaguchi, S. *et al.* The zinc-finger protein MAZR is part of the transcription factor network that controls the CD4 versus CD8 lineage fate of double-positive thymocytes. *Nat. Immunol.* **11**, 442–448 (2010).
14. Sun, G. *et al.* The zinc finger protein cKrox directs CD4 lineage differentiation during intrathymic T cell positive selection. *Nat. Immunol.* **6**, 373–381 (2005).
15. He, X. *et al.* The zinc finger transcription factor Th-POK regulates CD4 versus CD8 T-cell lineage commitment. *Nature* **433**, 826–833 (2005).
16. Muroi, S. *et al.* Cascading suppression of transcriptional silencers by ThPOK seals helper T cell fate. *Nat. Immunol.* **9**, 1113–1121 (2008).
17. Kovalovsky, D. *et al.* The BTB-zinc finger transcriptional regulator PLZF controls the development of invariant natural killer T cell effector functions. *Nat. Immunol.* **9**, 1055–1064 (2008).
18. Alonzo, E.S. *et al.* Development of promyelocytic zinc finger and ThPOK-expressing innate gamma delta T cells is controlled by strength of TCR signaling and Id3. *J. Immunol.* **184**, 1268–1279 (2010).
19. Savage, A.K. *et al.* The transcription factor PLZF directs the effector program of the NKT cell lineage. *Immunity* **29**, 391–403 (2008).
20. Kreslavsky, T. *et al.* TCR-inducible PLZF transcription factor required for innate phenotype of a subset of gammadelta T cells with restricted TCR diversity. *Proc. Natl. Acad. Sci. USA* **106**, 12453–12458 (2009).
21. Dent, A.L., Shaffer, A.L., Yu, X., Allman, D. & Staudt, L.M. Control of inflammation, cytokine expression, and germinal center formation by BCL-6. *Science* **276**, 589–592 (1997).
22. Ye, B.H. *et al.* The BCL-6 proto-oncogene controls germinal-centre formation and Th2-type inflammation. *Nat. Genet.* **16**, 161–170 (1997).
23. Yu, D. *et al.* The transcriptional repressor Bcl-6 directs T follicular helper cell lineage commitment. *Immunity* **31**, 457–468 (2009).
24. Johnston, R.J. *et al.* Bcl6 and Blimp-1 are reciprocal and antagonistic regulators of T follicular helper cell differentiation. *Science* **325**, 1006–1010 (2009).
25. Nurieva, R.I. *et al.* Bcl6 mediates the development of T follicular helper cells. *Science* **325**, 1001–1005 (2009).
26. Bezman, N.A. *et al.* Molecular definition of the identity and activation of natural killer cells. *Nat. Immunol.* **13**, 1000–1009 (2012).
27. Bukowski, J.F., Warner, J.F., Dennert, G. & Welsh, R.M. Adoptive transfer studies demonstrating the antiviral effect of natural killer cells in vivo. *J. Exp. Med.* **161**, 40–52 (1985).
28. Omori, M. *et al.* CD8 T cell-specific downregulation of histone hyperacetylation and gene activation of the IL-4 gene locus by ROG, repressor of GATA. *Immunity* **19**, 281–294 (2003).
29. Piazza, F., Costoya, J.A., Merghoub, T., Hobbs, R.M. & Pandolfi, P.P. Disruption of PLZP in mice leads to increased T-lymphocyte proliferation, cytokine production, and altered hematopoietic stem cell homeostasis. *Mol. Cell. Biol.* **24**, 10456–10469 (2004).
30. Miaw, S.C., Choi, A., Yu, E., Kishikawa, H. & Ho, I.C. ROG, repressor of GATA, regulates the expression of cytokine genes. *Immunity* **12**, 323–333 (2000).
31. Hirahara, K. *et al.* Repressor of GATA regulates TH2-driven allergic airway inflammation and airway hyperresponsiveness. *J. Allergy Clin. Immunol.* **122**, 512–520 (2008).
32. Hirasaki, Y. *et al.* Repressor of GATA negatively regulates murine contact hypersensitivity through the inhibition of type-2 allergic responses. *Clin. Immunol.* **139**, 267–276 (2011).
33. Miaw, S.C., Kang, B.Y., White, I.A. & Ho, I.C. A repressor of GATA-mediated negative feedback mechanism of T cell activation. *J. Immunol.* **172**, 170–177 (2004).
34. Marrack, P. & Kappler, J. Control of T cell viability. *Annu. Rev. Immunol.* **22**, 765–787 (2004).
35. Dunkle, A., Dzhagalov, I., Gordy, C. & He, Y.W. Transfer of CD8+ T cell memory using Bcl-2 as a marker. *J. Immunol.* **190**, 940–947 (2013).
36. Stergachis, A.B. *et al.* Developmental fate and cellular maturity encoded in human regulatory DNA landscapes. *Cell* **154**, 888–903 (2013).
37. Sun, J.C. *et al.* Proinflammatory cytokine signaling required for the generation of natural killer cell memory. *J. Exp. Med.* **209**, 947–954 (2012).
38. Miyagi, T. *et al.* High basal STAT4 balanced by STAT1 induction to control type 1 interferon effects in natural killer cells. *J. Exp. Med.* **204**, 2383–2396 (2007).
39. Hesslein, D.G. & Lanier, L.L. Transcriptional control of natural killer cell development and function. *Adv. Immunol.* **109**, 45–85 (2011).
40. Crotty, S., Johnston, R.J. & Schoenberger, S.P. Effectors and memories: Bcl-6 and Blimp-1 in T and B lymphocyte differentiation. *Nat. Immunol.* **11**, 114–120 (2010).
41. Kallies, A. *et al.* A role for Blimp1 in the transcriptional network controlling natural killer cell maturation. *Blood* **117**, 1869–1879 (2011).
42. Yoon, H.S. *et al.* ZBTB32 Is an Early Repressor of the CIITA and MHC Class II Gene Expression during B Cell Differentiation to Plasma Cells. *J. Immunol.* **189**, 2393–2403 (2012).
43. Shin, H.M. *et al.* Epigenetic modifications induced by Blimp-1 Regulate CD8(+) T cell memory progression during acute virus infection. *Immunity* **39**, 661–675 (2013).
44. Bikoff, E.K., Morgan, M.A. & Robertson, E.J. An expanding job description for Blimp-1/PRDM1. *Curr. Opin. Genet. Dev.* **19**, 379–385 (2009).
45. Sakurai, N. *et al.* The LRF transcription factor regulates mature B cell development and the germinal center response in mice. *J. Clin. Invest.* **121**, 2583–2598 (2011).
46. Phan, R.T. & Dalla-Favera, R. The BCL6 proto-oncogene suppresses p53 expression in germinal-centre B cells. *Nature* **432**, 635–639 (2004).
47. Phan, R.T., Saito, M., Basso, K., Niu, H. & Dalla-Favera, R. BCL6 interacts with the transcription factor Miz-1 to suppress the cyclin-dependent kinase inhibitor p21 and cell cycle arrest in germinal center B cells. *Nat. Immunol.* **6**, 1054–1060 (2005).
48. Tunyaplin, C. *et al.* Direct repression of prdm1 by Bcl-6 inhibits plasmacytic differentiation. *J. Immunol.* **173**, 1158–1165 (2004).
49. Vasanwala, F.H., Kusam, S., Toney, L.M. & Dent, A.L. Repression of AP-1 function: a mechanism for the regulation of Blimp-1 expression and B lymphocyte differentiation by the B cell lymphoma-6 protooncogene. *J. Immunol.* **169**, 1922–1929 (2002).
50. Lopez-Verges, S. *et al.* Expansion of a unique CD57(+)NKG2Chi natural killer cell subset during acute human cytomegalovirus infection. *Proc. Natl. Acad. Sci. USA* **108**, 14725–14732 (2011).
51. Foley, B. *et al.* Cytomegalovirus reactivation after allogeneic transplantation promotes a lasting increase in educated NKG2C+ natural killer cells with potent function. *Blood* **119**, 2665–2674 (2012).
52. Foley, B. *et al.* Human cytomegalovirus (CMV)-induced memory-like NKG2C(+) NK cells are transplantable and expand in vivo in response to recipient CMV antigen. *J. Immunol.* **189**, 5082–5088 (2012).
53. Romee, R. *et al.* Cytokine activation induces human memory-like NK cells. *Blood* **120**, 4751–4760 (2012).

ONLINE METHODS

Mice. Mice were bred at Memorial Sloan-Kettering Cancer Center in accordance with the guidelines of the Institutional Animal Care and Use Committee (IACUC). The following strains were used in this study: C57BL/6 (CD45.2$^+$; The Jackson Laboratory), B6.SJL (CD45.1$^+$; Taconic), *Rag2*$^{-/-}$*Il2rg*$^{-/-}$ (Taconic), *Il18r1*$^{-/-}$ (ref. 54), *Il12rb2*$^{-/-}$ (ref. 55), *Stat4*$^{-/-}$ (ref. 56), *Ifnar1*$^{-/-}$(ref. 57), *Klra8*$^{-/-}$ (Ly49H-deficient)[58], *B2m*$^{-/-}$ (Taconic), m157 transgenic[59], *Nkp46*^{iCre} (here called *Nkp46-Cre*)[60], *Prdm1*$^{fl/fl}$ (ref. 61) and *Zbtb32*$^{-/-}$ (ref. 31) mice. Femurs from *Il12rb2*$^{-/-}$ × *Ifnar1*$^{-/-}$ mice were provided by S. Way (University of Minnesota) for making mixed bone marrow chimeras. *Zbtb32*$^{-/-}$*Prdm1*$^{fl/fl}$ *Nkp46*$^{iCre/WT}$ animals and littermate controls were generated by breeding at Memorial Sloan-Kettering Cancer Center. Experiments were conducted without blinding using age- and gender-matched mice in accordance with approved institutional protocols.

Mixed bone marrow chimeric mice were generated as described[8]. Briefly, host C57BL/6 × B6.SJL animals (CD45.1$^+$CD45.2$^+$) were lethally irradiated with 900 grays of radiation and reconstituted with a 1:1 mixture of bone marrow cells from B6.SJL wild-type (WT) (CD45.1$^+$) and knockout donor (CD45.2$^+$) mice, coinjected with anti-NK1.1 (clone PK136) to deplete any residual donor or host mature NK cells. CD45.1$^+$CD45.2$^+$ host NK cells were excluded from all analyses.

Virus infections. MCMV (Smith strain) and MCMVΔm157 were obtained from L. Lanier (University of California San Francisco) and U. Koszinowski (Max von Pettenkofer Institute), respectively. MCMV was passaged serially through BALB/c hosts two times, then viral stocks were prepared by using a dounce homogenizer to dissociate the salivary glands of infected mice 3 weeks after infection. For neonate protection studies, 4-d-old Ly49H-deficient neonates received 10^6 WT or *Zbtb32*$^{-/-}$ Ly49H$^+$ NK cells by intraperitoneal (i.p.) injection and were infected by i.p. injection of 2×10^3 plaque-forming units (PFU) of MCMV on the following day. WT, *Zbtb32*$^{-/-}$ and mixed bone marrow chimera mice were infected by i.p. injection of 7.5×10^3 PFU of MCMV. For the adoptive transfer studies, mice were infected by i.p. injection of 7.5×10^2 PFU of MCMV one day after receiving approximately 1×10^6 Ly49H$^+$ NK cells by intravenous (i.v.) injection.

VSV-Indiana and recombinant VSV-m157, made by cloning the coding sequence for the MCMV glycoprotein m157 into the parental VSV-Indiana strain[62] were provided by K. Schluns (MD Anderson). For the VSV protection studies, adult Ly49H-deficient mice were infected by i.v. injection of 1.5×10^9 PFU of VSV-m157 1 d after receiving 1×10^6 WT or *Zbtb32*$^{-/-}$ Ly49H$^+$ NK cells by i.v. injection. In other adoptive transfer experiments, mice were infected by i.v. injection of 1×10^7 PFU of VSV-m157 or VSV-Indiana one day after receiving ~1×10^6 Ly49H$^+$ NK cells by i.v. injection.

VacV-m157 was provided by G. Gasteiger (Memorial Sloan-Kettering Cancer Center) and animals were infected by i.p. injection with 1×10^7 PFU.

Flow cytometry and cell sorting. Cell surface staining was performed using the following fluorophore-conjugated antibodies (purchased from BD Biosciences, eBioscience, BioLegend and R&D Systems): NK1.1 (PK136), CD11b (M1/70), CD27 (LG.3A10), CD49b/DX5 (DX5), KLRG1 (2F1), NKp46 (29A1.4), CD69 (H1.2F3), Ly49H (3D10), Granzyme B (16G6), CD107a (1D4B), CD45.1 (A20), CD45.2 (104), CD8α (53-6.7), CD122 (TM-β1), TCRβ (H57-597), CD3ε (145-2C11), IFN-γ (XMG1.2), Ly49D (4E5), Ly49A (A1/Ly49A), Ly49C/I (5E6), T-bet (4B10), Bcl-2 (3F11), Ki67 (B56), GATA-3 (L50-823), STAT-pY701 (4a), STAT-pY705 (4/P-STAT3), STAT-pY693 (38/p-STAT) and peptide-loaded MHC class I tetramers (MCMV peptides m45, m38 or m139; NIH Tetramer Facility). Unless otherwise indicated, NK cells were defined as TCRβ$^-$NK1.1$^+$ or CD3$^-$NK1.1$^+$ cells. Intracellular staining was performed by fixing and permeabilizing with the Foxp3/Transcription Factor Staining Kit (eBioscience) for staining intranuclear proteins, including Zbtb32; with Cytofix/Cytoperm Plus (BD) for staining cytokines; or with formaldehyde and methanol for staining phosphorylated STAT proteins. For the detection of intracellular Zbtb32, permeabilized cells were stained with 4 μg/ml of a rat anti-Zbtb32 primary antibody (#853111, provided by R&D Systems) for 45 min at 4 °C, then with a FITC-conjugated anti-rat secondary antibody for 10 min at 4 °C. Pan-caspase staining was carried out using the FAM FLICA *in vitro* Poly Caspase Kit (Immunochemistry Technologies) per the manufacturer's instructions. Positive control cells were first incubated with 20 μg/ml of anti-mouse CD95 (clone Jo-2; BD Pharmingen) for 2.5–4 h at 37 °C (data not shown). For the BrdU labeling experiments, mice were subjected to i.p. injection of 1.5 mg of BrdU in PBS on days 3.5 and 5.5 after infection with MCMV, and BrdU labeling was determined ~16 h later using the APC BrdU Flow Kit (BD Biosciences).

Flow cytometry and cell sorting were performed on the LSR II and Aria II cytometers (BD Biosciences), respectively. For experiments involving qRT-PCR, cell populations were sorted to >95% purity. Data were analyzed with FlowJo software (Tree Star).

NK cell enrichment and adoptive transfer. T, B, and red blood cells were labeled with 10 μg per spleen of rat monoclonal antibodies against CD4 (GK1.5), CD8 (53.6.72), CD19 (1D3) and Ter119 (obtained from the UCSF Core Facility) and magnetically depleted from total splenocyte suspensions using anti-rat IgG–coupled magnetic beads (Qiagen)[37]. ~10^6 enriched NK cells (typically 25–70% of the total cells) were i.v. injected into adult or i.p. injected into neonate recipients 1 d before infection. For experiments involving adoptive cotransfer of CD45.1$^+$ and CD45.2$^+$ populations, equal numbers of Ly49H$^+$ NK cells from each population were cotransferred together into recipients 1 d before infection. In some experiments, splenocytes were labeled before transfer with 5 μM Vybrant CFDA (Molecular Probes).

***Ex vivo* stimulation of NK cells.** ~10^5 sorted NK cells were stimulated for 18 h in RPMI containing 5% FBS with recombinant mouse IL-12 (20 ng/ml; R&D Systems), IL-18 (10 ng/ml; R&D Systems), or IFN-α/β (400 U/ml) or with plate-bound antibodies (10 μg/ml; eBioscience) against the activating NK cell receptors Ly49H (3D10), Ly49D (4E5), NKp46 (29A1.4) or NK1.1 (PK136).

For *ex vivo* NK cell expansion experiments, 2.5×10^5 sorted NK cells (>98% purity) were stimulated in RPMI supplemented with 10% FBS, penicillin-streptomycin, L-glutamine and β-mercaptoethanol, and containing recombinant mouse IL-2 (20 ng/ml; R&D Systems) and IL-15 (40 ng/ml; R&D Systems). Fresh medium and cytokines were added on alternating days of culture.

Quantitative reverse-transcription PCR. Cells were lysed in Tri-Reagent (Ambion). RNA purification and cDNA synthesis were carried out with the Qiagen RNeasy kit (with on-column DNase I treatment), and MuLV reverse transcriptase and oligo(dT)$_{16}$ primers (Applied Biosystems). iQ Sybr Green SuperMix (BioRad) was used for qRT-PCR. Data were normalized to that for *Actb* and expressed as relative target abundance via the ΔΔCt method, where Ct (threshold cycle) is the cycle number at which the amplification curve intersects the threshold value. **Supplementary Table 1** lists relevant primer sequences. For data in **Figure 5d**, the Mouse Cell Cycle PCR Array, RT^2 SYBR Green qPCR Master Mix and Mouse Cell Cycle RT^2 PreAMP cDNA synthesis kits (Qiagen) were used.

Chromatin immunoprecipitation. ~5×10^6 enriched splenic NK cells were purified by sorting on TCRβ$^-$NK1.1$^+$ cells. Proteins were cross-linked to DNA for 8 min at 25 °C by addition of 1% formaldehyde to the medium. ChIP was carried out as previously described[63] using 10 μg of rabbit polyclonal anti-STAT4 (Santa Cruz, sc-468, clone C-20) or 10 μg of rabbit serum IgG antibody as a control (data not shown; Sigma, I5006), or 0.5 μg of anti-H3K27Ac (Abcam, 4729). Relative abundance of regulatory sequences in the *Zbtb32* promoter or, as controls, in the *Actb* and *Gapdh* promoters or a 'gene desert' ~50 kb upstream of the *Foxp3* gene was measured by qPCR in the antibody-precipitated DNA using iQ Sybr Green SuperMix (BioRad). After determining the Ct value, percent input was calculated as $100 \times 2^{(\text{Ct adjusted input} - \text{Ct target})}$, where the Ct^{input} was adjusted from 5% to 100% by subtracting $\log_2$ 20 Ct values. Primer sequences are listed in **Supplementary Table 2**.

Statistical analyses. For graphs, data are shown as mean ± s.e.m. and, unless otherwise indicated, statistical differences were evaluated using a two-tailed unpaired Student's *t*-test, assuming equal sample variance. $P < 0.05$ was considered significant. Statistical differences in survival were determined by Gehan-Breslow-Wilcoxon Test analysis. Graphs were produced and statistical analyses were performed using GraphPad Prism. Sample size was not specifically predetermined, but the number of mice used was consistent with prior experience with similar experiments.

doi:10.1038/ni.2876

54. Hoshino, K. *et al.* Cutting edge: generation of IL-18 receptor-deficient mice: evidence for IL-1 receptor-related protein as an essential IL-18 binding receptor. *J. Immunol.* **162**, 5041–5044 (1999).
55. Wu, C. *et al.* IL-12 receptor beta 2 (IL-12R beta 2)-deficient mice are defective in IL-12-mediated signaling despite the presence of high affinity IL-12 binding sites. *J. Immunol.* **165**, 6221–6228 (2000).
56. Kaplan, M.H., Sun, Y.L., Hoey, T. & Grusby, M.J. Impaired IL-12 responses and enhanced development of Th2 cells in Stat4-deficient mice. *Nature* **382**, 174–177 (1996).
57. Muller, U. *et al.* Functional role of type I and type II interferons in antiviral defense. *Science* **264**, 1918–1921 (1994).
58. Fodil-Cornu, N. *et al.* Ly49h-deficient C57BL/6 mice: a new mouse cytomegalovirus-susceptible model remains resistant to unrelated pathogens controlled by the NK gene complex. *J. Immunol.* **181**, 6394–6405 (2008).
59. Tripathy, S.K. *et al.* Continuous engagement of a self-specific activation receptor induces NK cell tolerance. *J. Exp. Med.* **205**, 1829–1841 (2008).
60. Narni-Mancinelli, E. *et al.* Fate mapping analysis of lymphoid cells expressing the NKp46 cell surface receptor. *Proc. Natl. Acad. Sci. USA* **108**, 18324–18329 (2011).
61. Shapiro-Shelef, M. *et al.* Blimp-1 is required for the formation of immunoglobulin secreting plasma cells and pre-plasma memory B cells. *Immunity* **19**, 607–620 (2003).
62. Kim, S.K. *et al.* Generation of mucosal cytotoxic T cells against soluble protein by tissue-specific environmental and costimulatory signals. *Proc. Natl. Acad. Sci. USA* **95**, 10814–10819 (1998).
63. Zheng, Y. *et al.* Genome-wide analysis of Foxp3 target genes in developing and mature regulatory T cells. *Nature* **445**, 936–940 (2007).